Real-time one-dimensional coherent imaging through single-mode fibers by space–time conversion processors

P. C. Sun, Y. T. Mazurenko,* and Y. Fainman

Department of Electrical and Computer Engineering, University of California, San Diego, La Jolla, California 92093-0407

Received June 26, 1997

We introduce and experimentally demonstrate a novel technique for one-dimensional coherent imaging through a single-mode optical fiber by use of a pulse shaper and a pulse imager. In contrast to the wavelength-division-multiplexed encoding technique, our approach preserves both amplitude and phase information of the optical signal transmitted through the fiber, allowing one to encode longitudinal in addition to transverse optical information. The effect of the fiber-material dispersion on our imaging technique is analyzed, and potential solutions are discussed. © 1997 Optical Society of America

Transmission of a complex-amplitude one-dimensional (1D) parallel data array or a 1D image through a single-mode fiber is an important but challenging task, because the small entrance pupil of an optical fiber limits coupling of the signal's spatial modes. A common approach to such transmission uses wavelength-division multiplexing,[1–3] which encodes spatial information directly onto the different spectral components of a broadband point source. The idea of wavelength-division multiplexing is simple, but since it is an incoherent technique, only magnitude information on the complex-amplitude spatial signal can be transmitted. In contrast, a coherent technique would transmit both the amplitude and the phase of a 1D complex-amplitude signal. Lukosz[4] introduced a technique combining the temporal and the spatial-frequency bandwidths, resulting in an optical system that permits resolution exceeding that permitted by the system's aperture. This superresolution approach is capable of sending complex-amplitude signals over a diffraction-limited aperture (e.g., a single-mode fiber) by holographic recording and reconstruction of the complex signals at the receiver.[5,6] However, the requirement of reconstructing images from a hologram prevents real-time data transmission. In this Letter we present a novel approach that combines the advantages of both wavelength-division multiplexing and Lukosz's superresolution technique, permitting real-time parallel transmission of 1D complex-amplitude signals through a single-mode optical fiber. Further, we demonstrate experimentally that this technique is capable of transmitting, through a single-mode fiber, image-depth information encoded on the input optical signals.

Our approach uses a pair of space–time conversion processors (see Fig. 1), a femtosecond pulse shaper[7,8] at the transmitter, and a femtosecond pulse imager[9,10] at the receiver. The pulse shaper is designed to be analogous to a coherent spatial Fourier optics 4-F filtering system. The pulse-shaper system shown in Fig. 1(a) consists of a pair of spectrum-decomposition devices (G1–L1 and G2–L2) in combination with a spectral-domain filter. The desired pulse shape at the output is obtained by use of a properly designed complex-amplitude spatial filter in the spectral domain to modulate the complex amplitude of the temporal-frequency spectrum of an incident transform-limited pulse. The spectral filter can be implemented with either a fixed[7,8] or a programmable mask[11] or can be prepared holographically, similarly to a Vander-Lugt filter.[12] Note that the Fourier spectral filter has to be updated at very high speed to achieve real-time operation. Current research on using photorefractive multiple-quantum-well devices for pulse shaping may provide a solution for this requirement.[13] The shaped pulse from the transmitter [see Fig. 1(a)] is sent through a single-mode optical fiber to the receiver [see Fig. 1(b)], where a pulse imager is employed to convert the temporal information of the shaped pulse back into the spatial domain. This conversion is based on nonlinear-optical three-wave mixing of the spatially spread and inverted temporal spectrum of the shaped and the reference pulses.[10]

In the experiment we use pulses of 200 fs at a 920-nm center wavelength, generated from a mode-locked Ti:sapphire laser (Mira 900; Coherent, Inc.). The laser output is expanded, collimated, and then split into two beams. The first beam is used as a

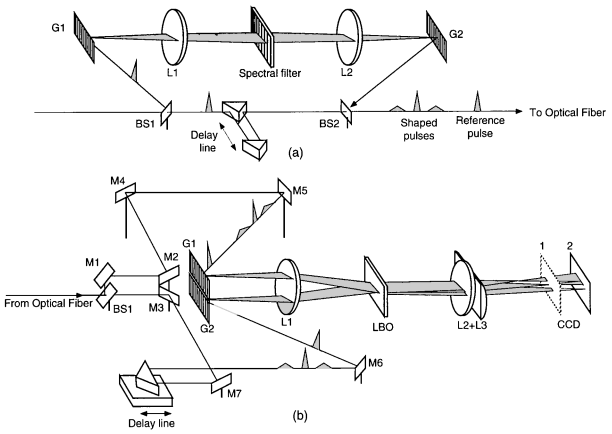

Fig. 1. Schematic diagram of optical processors for imaging through a single-mode fiber. (a) Pulse shaper: G1, G2, gratings; L1–L3, lenses; BS1, BS2, beam splitters. (b) Pulse imager: M1–M7, mirrors; LBO, LiB_3O_5; 1, 2, image planes.

0146-9592/97/241861-03$10.00/0

reference beam (or clock pulse), and the second beam is used as a transform-limited input pulse to the pulse-shaping device shown in Fig. 1(a). We then combine the shaped output pulse and the reference pulse beams collinearly in space but separate them in time to avoid interference. These collinear beams are guided into a 1-m-long single-mode fiber and transmitted to the receiver.

At the receiver [see Fig. 1(b)], the beam exiting from the fiber is passed through a polarization compensator to restore its original polarization. The polarization-compensated fiber output is then split into two beams, both consisting of the shaped and the reference pulses. These two beams are then introduced into the pulse imager. The pulse-imager setup is similar to that of Ref. 10, in which a nonlinear-optical LBO crystal (Super Technology, Inc.) was used in the Fourier transform plane of a three-wave mixing arrangement. The delay line in the second beam is used to synchronize the shaped pulse from the first beam and the reference pulse from the second beam such that they appear simultaneously on the LBO crystal, generating the output second-harmonic field. The generated second-harmonic field propagates in a vertical bisector direction, which coincides with the optical axis of the system. A horizontal slit, a Glan–Thompson polarizer, and a narrow-band color filter provide three stages of filtering for separation of the second-harmonic signal from the fundamental-frequency light of the two input beams. An anamorphic imaging system (L2–L3) performs a spatial Fourier transform in the horizontal direction and images in the vertical direction, producing an output pulse image detected by a CCD camera.

In our initial experiment on transmitting a 1D image through a single-mode fiber, we used a 50/50 binary amplitude grating (i.e., a Ronchi grating) as the spectral filter in the pulse-shaping device. The Fraunhofer diffraction pattern of such a grating does not have even diffraction orders, except for the zeroth order. From the experimental results we obtain the intensity profile [see Fig. 2(a)] of the pulse image, which clearly shows that the even-order pulses in the sequence (beside the zeroth order) do not appear. The three central pulses (i.e., -1, 0, and $+1$ orders) are close together, whereas the pulses that correspond to higher orders are separated by twice the distance. This experimental result demonstrates the capability of our system of performing parallel 1D imaging through a single-mode fiber.

In the second experiment we used a pulse shaper with a spectral filter implemented by an off-axis 1D binary-phase diffractive lens. We designed the off-axis diffractive lens to produce uniform diffraction efficiencies for the -1, 0, and $+1$ diffractive orders, which correspond to a negative quadratic-phase, a constant-phase, and a positive quadratic-phase function, respectively. The pulse-shaper output consists of a sequence of three temporally separated negative chirped, transform-limited, and positive chirped pulses, corresponding to the -1, 0, and $+1$ diffraction orders, respectively. Figure 2(b) shows the pulse image recorded by the CCD camera located in the exact image plane of the pulse imager [plane 1 of Fig. 1(b)]. As expected, the detected image consists of three pulses: a transform-limited pulse in the middle of the images of the positive and the negative chirped pulses. The images of the positive and the negative chirped pulses are asymmetric and weaker in amplitude than the transform-limited pulse as a result of angular dependence of the field coupling into single-mode optical fibers. When the CCD camera is translated backward in the longitudinal direction to plane 2 of Fig. 1(b), the image corresponding to the negative chirped pulse becomes narrower, with a width corresponding to that of a transform-limited pulse, and the other two pulses become wider [see Fig. 2(c)]. This phenomenon is known as space–time duality, which implies that the group-velocity dispersion in the temporal domain is equivalent to the Fresnel diffraction in the spatial domain.[14] Figure 2(c) also shows that

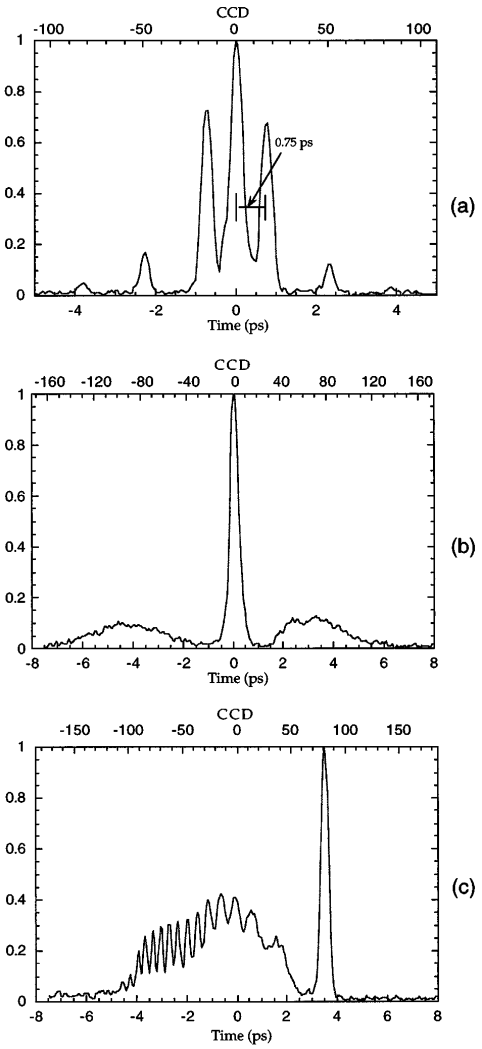

Fig. 2. Experimental results of 1D image transmission through a single-mode fiber: (a) intensity profile of a shaped-pulse image generated by a pulse shaper with a spectral filter implemented by a Ronchi grating, (b) intensity profile of a shaped-pulse image generated by a pulse shaper with a spectral filter implemented by a 1D diffractive lens, and (c) the same shaped-pulse image as in (b) but recorded in a longitudinally shifted observation plane where the negative chirped pulse is focused.

the generated second-harmonic fields that correspond to the different shaped pulses can interfere with each other, indicating that the second-harmonic field is quasi-monochromatic and coherent.

Material dispersion can affect the performance of our technique for real-time imaging through the fiber. In principle, the introduced group dispersion can be compensated for by a pulse shaper at the receiver or by use of a dispersion-compensation fiber.[15] Since our technique uses transmission of both the shaped and the reference pulses through the same single-mode optical fiber, shapes of both pulses will be affected identically (assuming that there are linear effects). Therefore the shaped and the reference pulses transmitted through such a fiber can be described as

$$u_{s,r}^{(o)}(t) = F_\omega[U_{s,r}^{(i)}(\omega)M(\omega)] = u_{s,r}^{(i)}(t) \otimes m(t), \quad (1)$$

where F_ω denotes the temporal-frequency Fourier-transform operator; superscripts i and o are the input and the output of the optical fiber, respectively; subscripts s and r are the shaped and the reference pulses, respectively; $u_{s,r}^{(i)}(t)$ and $U_{s,r}^{(i)}(\omega)$ are the time (t) signal and the corresponding temporal-frequency (ω) spectrum, respectively; and $m(t)$ and $M(\omega)$ are the impulse response and the temporal-frequency transfer function of the optical fiber, respectively. Note that in Eq. (1) we discount the carrier frequency of the short pulse, which means that the temporal-frequency spectrum is centered at the carrier frequency of the short pulse. The transfer function of the optical fiber can be described by

$$M(\omega) = \exp[-jk(\omega)L] = \exp\left[-j\left(\sum_n \omega^n k_n\right)L\right], \quad (2)$$

where $k(\omega)$ is the propagation constant for each spectral component of the pulses propagating in the optical fiber, L is the length of the optical fiber, and the right-hand side is obtained with a Taylor series expansion of $k(\omega)$ with coefficient k_n. Next we consider the effect of introducing the shaped and the reference pulses from the fiber output into the pulse-imaging system of Fig. 1(b). The shaped-pulse image is determined by the spatial Fourier transform of the second-harmonic field, which in turn is proportional to the product of the inverted signal and the reference-spectrum amplitudes at the receiver [see also Eq. (18) of Ref. 10]:

$$\begin{aligned} u_{\mathrm{img}}(x) &= F_\omega[U_s^{(i)}(-\omega)M(-\omega)U_r^{(i)}(\omega)M(\omega)]_{t=\gamma x} \\ &= F_\omega\{U_s(-\omega)U_r(\omega)\exp[-j2(k_2\omega^2 \\ &\quad + k_4\omega^4 + k_6\omega^6 + \ldots)L]\}_{t=\gamma x} \\ &= \{[u_s^{(i)}(-\gamma x) \otimes u_r^{(i)}(\gamma x)] \otimes h(\gamma x)\} \\ &\quad \otimes \exp\left(j\frac{\gamma^2 x^2}{8k_2 L}\right), \end{aligned} \quad (3)$$

where γ accounts for the time–space conversion (i.e., $t = \gamma x$), $\otimes$ denotes the convolution operator, we neglect constant phase, and $h(\gamma x)$ represents the impulse–response function of all dispersion components larger than $n \geq 4$ order. We observed from Eq. (3) that only the even-order terms of the Taylor expansion of the propagation constant can affect the result of the pulse-imaging system, whereas all the odd-order terms are canceled out. The result of Eq. (3) also indicates that the second-order effect of the group-velocity dispersion from the optical fiber can be eliminated by a longitudinal translation of the image-observation plane by a distance $z = 8\pi k_2 L/\lambda_c \gamma^2$, where λ_c is the center wavelength of the pulse beam. In the new observation plane the image of the shaped pulse transmitted through the dispersive fiber will be identical to that obtained without group dispersion, assuming negligible higher-order dispersion coefficients [i.e., $h(\gamma x) = \delta(x)$]. Furthermore, when the effects of high-order dispersions cannot be neglected, they can easily be compensated for in the spatial domain by properly designed fixed or programmable phase masks, because the time-domain dispersion effects have been transferred into the spatial domain and act as spatial aberrations.

This study was supported in part by the Focused Research Initiative of Ballistic Missile Defense Organization, the U.S. Air Force Office of Scientific Research, and the National Science Foundation. Y. Mazurenko acknowledges support from the Russian Foundation for Fundamental Research.

*Permanent address, S. I. Vavilov State Optical Institute, St. Petersburg 199034, Russia.

References

1. J. D. Armitage, A. Lohmann, and D. P. Paris, Jpn. J. Appl. Phys. **4,** 273 (1965).
2. E. G. Paek, C. E. Zah, K. W. Cheung, and L. Curtis, Opt. Lett. **17,** 613 (1992).
3. E. A. De Souza, M. C. Nuss, W. H. Knox, and D. A. B. Miller, Opt. Lett. **20,** 1166 (1995).
4. W. Lukosz, J. Opt. Soc. Am. **57,** 932 (1967).
5. P. C. Sun and E. N. Leith, Appl. Opt. **10,** 4857 (1992).
6. P. Naulleau, M. Brown, C. Chen, and E. Leith, Opt. Lett. **21,** 36 (1996).
7. C. Froehly, B. Colombeau, and M. Vampouille, in *Progress in Optics*, E. Wolf, ed. (North-Holland, Amsterdam, 1983), Vol. XXII, p. 65.
8. A. M. Weiner, J. P. Heritage, and E. M. Kirschner, J. Opt. Soc. Am. B **5,** 1563 (1988).
9. Y. T. Mazurenko, A. G. Spiro, S. E. Putilin, A. G. Beliaev, and E. B. Verkhovskij, Opt. Commun. **118,** 594 (1995).
10. P. C. Sun, Y. T. Mazurenko, and Y. Fainman, J. Opt. Soc. Am. A **14,** 1159 (1997).
11. A. M. Weiner, D. E. Leaird, J. S. Patel, and J. R. Wullert, Opt. Lett. **15,** 326 (1990).
12. P. C. Sun, Y. Mazurenko, W. S. C. Chang, P. K. L. Yu, and Y. Fainman, Opt. Lett. **20,** 1728 (1995).
13. Y. Ding, R. M. Brubaker, D. D. Nolte, M. R. Melloch, and A. M. Weiner, Opt. Lett. **22,** 718 (1997).
14. B. H. Kolner and M. Nazarathy, Opt. Lett. **14,** 630 (1989).
15. C. C. Chang, A. M. Weiner, A. M. Vengsarkar, and D. W. Peckham, Opt. Lett. **21,** 1141 (1996).